Probing the Roles of Active Site Residues in Phosphatidylinositol-Specific Phospholipase C from *Bacillus cereus* by Site-Directed Mutagenesis†

Claudia S. Gässler,‡ Margret Ryan,§ Tun Liu,§ O. Hayes Griffith,§ and Dirk W. Heinz*,‡

Institut für Organische Chemie und Biochemie, Universität Freiburg, D-79104 Freiburg, Germany, and Institute of Molecular Biology, Department of Chemistry, University of Oregon, Eugene, Oregon 97403

Received May 12, 1997; Revised Manuscript Received July 23, 1997⊗

ABSTRACT: The role of amino acid residues located in the active site pocket of phosphatidylinositol-specific phospholipase C (PI-PLC) from *Bacillus cereus* [Heinz, D. W., Ryan, M., Bullock, T., & Griffith, O. H. (1995) *EMBO J. 14*, 3855−3863] was investigated by site-directed mutagenesis, kinetics, and crystal structure analysis. Twelve residues involved in catalysis and substrate binding (His32, Arg69, His82, Gly83, Lys115, Glu117, Arg163, Trp178, Asp180, Asp198, Tyr200, and Asp274) were individually replaced by 1−3 other amino acids, resulting in a total number of 21 mutants. Replacements in the mutants H32A, H32L, R69A, R69E, R69K, H82A, H82L, E117K, R163I, D198A, D198E, D198S, Y200S, and D274S caused essentially complete inactivation of the enzyme. The remaining mutants (G83S, K115E, R163K, W178Y, D180S, Y200F, and D274N) exhibited reduced activities up to 57% when compared with wild-type PI-PLC. Crystal structures determined at a resolution ranging from 2.0 to 2.7 Å for six mutants (H32A, H32L, R163K, D198E, D274N, and D274S) showed that significant changes were confined to the site of the respective mutation without perturbation of the rest of the structure. Only in mutant D198E do the side chains of two neighboring arginine residues move across the inositol binding pocket toward the newly introduced glutamic acid. An analysis of these structure−function relationships provides new insight into the catalytic mechanism, and suggests a molecular explanation of some of the substrate stereospecificity and inhibitor binding data available for this enzyme.

Phosphatidylinositol-specific phospholipase C (PI-PLC)[1] (EC 3.1.4.10) catalyzes the cleavage of the *sn*-3 phosphodiester bond of phosphatidylinositol (PI) into lipid-soluble diacylglycerol (DAG) and water-soluble inositol 1-phosphate [I(1)P, Figure 1). PI-PLCs are ubiquitous enzymes that are found in eukaryotic cells where they play a central role in PI signal transduction cascades by generating two second messenger molecules: diacylglycerol (DAG), which activates protein kinase C isozymes; and inositol 1,4,5-trisphosphate, which promotes the release of Ca^{2+} ions from internal stores (Berridge, 1993; Berridge & Irvine, 1989; Rhee et al., 1989). PI-PLCs are also secreted by a number of Gram-positive bacteria, *e.g.*, *Bacillus cereus* (Ikezawa et al., 1976), *Bacillus thuringiensis* (Ikezawa & Taguchi, 1981), *Staphylococcus aureus* (Low, 1981), *Clostridium novyi* (Taguchi & Ikezawa, 1978), and *Listeria monocytogenes* (Leimeister-Wächter et al., 1991; Mengaud et al., 1991). The physiological roles of the bacterial enzymes are not well understood, although it has been suggested that the PI-PLCs are virulence factors in the human pathogens *L. monocytogenes* and *S. aureus* (Leimeister-Wachter et al., 1991; Mengaud et al., 1991; Camilli et al., 1991; Daugherty & Low, 1993). The bacterial PI-PLCs but not the mammalian isozymes cleave proteins tethered to membranes by glycosylphosphatidylinositol (GPI) anchors, and they are widely used in tests for and isolation of GPI-linked proteins (Low & Saltiel, 1988; Ferguson & Williams, 1988).

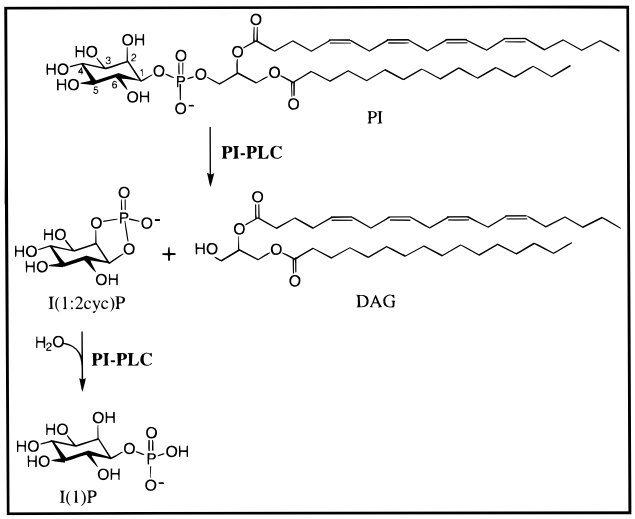

FIGURE 1: Reactions catalyzed by *B. cereus* PI-PLC. The first step is an intrinsic phosphotransfer reaction, leading to the formation of I(1:2cyc)P and DAG. Both of these compounds are released as products. In a second, much slower step, the enzyme catalyzes the hydrolysis of I(1:2cyc)P to form I(1)P.

† This work was supported by the Deutsche Forschungsgemeinschaft and Land Baden-Württemberg to D.W.H., and by NIH Grant GM25698 to O.H.G.

* Author to whom correspondence should be addressed.

‡ Universität Freiburg.

§ University of Oregon.

⊗ Abstract published in *Advance ACS Abstracts*, September 15, 1997.

[1] Abbreviations: Mutant enzymes are designated by the single-letter code for the wild-type amino acid followed by the residue number and then the amino acid replacement, e.g., H32A; BSA, bovine serum albumin; DAG, 1,2-diacyl-*sn*-glycerol; DOC, deoxycholic acid, sodium salt; EDTA, ethylenediaminetetraacetic acid, disodium salt; GPI, glycosylphosphatidylinositol; HEPES, *N*-(2-hydroxyethyl)piperazine-*N*′-2-ethanesulfonic acid; Tris, tris(hydroxymethyl)aminomethane; I(1)P, D-*myo*-inositol 1-phosphate; I(1:2cyc)P, *myo*-inositol 1,2-cyclic phosphate; kbp, kilobase pair(s); NPIP, *myo*-inositol 1-(4-nitrophenyl phosphate); PI, phosphatidylinositol; PI-PLC, phosphatidylinositol-specific phospholipase C; pNP, *p*-nitrophenolate.

S0006-2960(97)01102-1 CCC: $14.00

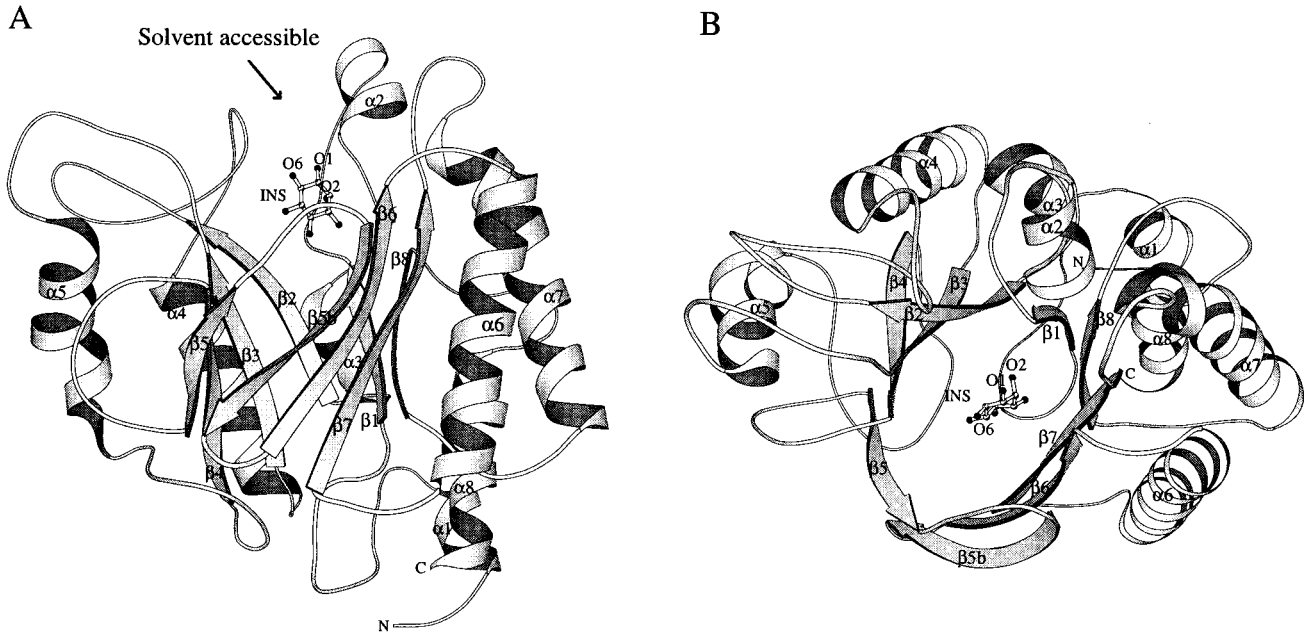

FIGURE 2: Ribbon diagram of the structure of *B. cereus* PI-PLC with *myo*-inositol (INS) bound at the active site. (A) Side view of the $(\beta\alpha)_8$-barrel. The active site is located at the C-termini of the strands of the barrel and is solvent-accessible. (B) Looking down the barrel. This view reveals an imperfect TIM barrel with helices missing between strands 5 and 6, which leaves this side of the barrel more open to the solvent. Interestingly, the 1-OH (O1) and 6-OH (O6) groups of inositol are pointing toward solvent from this side of the barrel. The 1-OH group is replaced by a phosphatidyl group in the natural substrates PI and GPI. The 6-OH group is replaced in GPI by a glucosaminyl group, which is attached to proteins that are to be located in membrane. This figure as well as Figures 4−7 are generated using Molscript (Kraulis, 1991).

In many ways the PI-PLCs from *B. cereus* and by implication the nearly identical enzyme from *B. thuringiensis* form an ideal model system for the study of this large class of enzymes, and they are the focus of considerable attention in the literature [for a review, see Bruzik and Tsai (1994)]. *B. cereus* PI-PLC is small (298 amino acid residues, 35 kDa), of moderate thermal stability, and metal-ion-independent, and consists of a single polypeptide with no disulfide bonds and is active as a monomer (Griffith et al., 1991). This enzyme shows a remarkable head-group specificity, recognizing and cleaving only PI and not phosphorylated derivatives of PI, or other common phospholipids such as phosphatidylcholine, phosphatidylserine, or sphingomyelin which are cleaved by different bacterial PLCs (Ikezawa & Taguchi, 1981). Even toward PI, *B. cereus* PI-PLC is highly selective. It preferentially cleaves phospholipids containing *myo*-inositol, which is only one of nine possible stereoisomers of inositol, and these enzymes have an absolute requirement for the 1D configuration of *myo*-inositol in PI (Leigh et al., 1992; Lewis et al., 1993; Bruzik & Tsai, 1994). *B. thuringiensis* PI-PLC also cleaves a phospholipid containing 1L-*chiro*-inositol, which is identical to 1D-*myo*-inositol except for inversion of the hydroxyl group at the 3 position, however at 103-fold reduced rates (Bruzik et al., 1994). In contrast to the strict head-group selectivity, the enzymes are not sensitive to other components of the substrate, e.g., the stereochemistry of the *sn*-2 carbon of the glycerol moiety (Bruzik & Tsai, 1994). Numerous variations in the lipid portion of the molecule are permitted; e.g., ether- or ester-linked lipids, mono- or diacyl lipids, or ceramides are good substrates (Guther et al., 1994).

PI-PLCs exhibit both phosphotransferase and cyclic phosphodiesterase activities, cleaving PI to form *myo*-inositol 1,2-cyclic phosphate, I(1:2cyc)P, which then is very slowly hydrolyzed to form *myo*-inositol 1-phosphate [I(1)P, Figure 1]. These two reactions are sequential in the bacterial enzymes, as established by ^{31}P NMR. The presence of the cyclic intermediate suggests a ribonuclease-like mechanism (Volwerk et al., 1990). The mechanism of eukaryotic PI-PLCs is more difficult to analyze. Experiments utilizing isotopically labeled phosphates indicate that *B. cereus* PI-PLC and mammalian PI-PLCs convert PI to I(1)P with overall retention of configuration at the phosphorus atom, supporting the idea that the mammalian as well as the bacterial PI-PLCs cleave PI to form the two products in sequential rather than in parallel reactions (Bruzik et al., 1992; Bruzik & Tsai, 1994).

The three-dimensional structure of PI-PLC from *B. cereus* has been determined by X-ray crystallography (Heinz et al., 1995). This enzyme consists of a single globular domain, an irregular $(\beta\alpha_8)$-barrel (TIM-barrel) with the active site located at the C-terminal end of the β-barrel (Figure 2). Based on the structure of *B. cereus* PI-PLC in complex with the competitive inhibitor *myo*-inositol, a catalytic mechanism of general base and acid catalysis utilizing two histidines in positions 32 and 82 was postulated (Heinz et al., 1995). Recently, an X-ray crystallographic structure of a multidomain mammalian PI-PLCδ_1 has been determined. The catalytic domain shows a highly similar topology when compared with the bacterial PI-PLC, in spite of low sequence homology (Essen et al., 1996). Studies of a series of substrate analogs in complex with the mammalian enzyme have provided additional evidence of the sequential mechanism, and further illustrate the close relationship between the bacterial and eukaryotic isozymes (Essen et al., 1997).

In this study, we focus on the relationship between the structure of *B. cereus* PI-PLC and its functional properties, with the aim of providing an understanding of the recognition of the *myo*-inositol head group, and the catalytic mechanism. Twenty-one individual mutants were constructed by site-

directed mutagenesis to systematically examine the role of amino acid residues located in the active site (Figure 3). A preliminary kinetic analysis of these mutants, using two different assays, and high-resolution crystal structures for some of the mutants are described. We show that the introduction of single amino acid replacements in the active site leads in most cases to a drastic decrease in catalytic activity despite the very localized nature of the structural change. Ratios of kinetic data from assays using the natural and a synthetic substrate provide a better understanding of the roles of the catalytic histidines. The surprisingly low tolerance toward even conservative amino acid replacements in the active site pocket explains the observed exquisite substrate specificity, and allows the identification of additional amino acids involved in the catalytic mechanism. Finally, by examining stereoisomers of inositol modeled into the *myo*-inositol binding site, some insights are gained in support of substrate and inhibitor binding specificities of *B. cereus* PI-PLC.

MATERIALS AND METHODS

Materials. Tritium-labeled PI, L-[*myo-inositol*-2-^{3}H(N)]-phosphatidylinositol, was from Du Pont NEN Research Products, and unlabeled PI from bovine liver (sodium salt; Avanti Polar Lipids, Inc.) or wheat germ (sodium salt, ICN) was purchased as the lyophilized powder. BSA was from Serva or USB; Tris base, PEG of average MW 8000, and *p*-nitrophenol were from Sigma. EDTA was obtained from Serva or International Biotechnologies, Inc. HEPES and DOC were purchased from Calbiochem; DOC was also obtained from Sigma.

Construction of Mutants. Single amino acid substitutions were introduced into *B. cereus* PI-PLC using the PI-PLC overexpression vector pHS475 and either the Chameleon double-stranded site-directed mutagenesis kit (Stratagene), or the Eckstein method (Sculptor *in vitro* mutagenesis system RPN 1526; Amersham), following the procedures recommended by the manufacturers or by the Kunkel method (Kunkel et al., 1987). The construct pHS475 is identical to plasmid pIC (Koke et al., 1991) except that about 3 kbp of noncoding *B. cereus* sequence have been deleted. The selection primer 5′-CATCATTGGAAAACGCTCTTCGGGGCG-3′ (Stratagene) was used to remove a unique *Xmn*I site.

The following mutagenic primers (Cruachem, Bio-Synthesis, Inc., or Pharmacia) were used and are listed 5′ to 3′ with the replaced bases underlined and the mutation produced in parentheses: GTCCCACTATCGGCTGTTCCTGG (H32A), GTCCCACTATCGAGTGTTCCTGG (H32L), GTTAAACGTCCTGCTATATCAAAAATG (R69A), GTTAAACGTCCTTCTATATCAAAAATG (R69E), GTTAAACGTCCCTTTATATCAAAAATG (R69K), GATATAATGGCCCAGCATGAAGAAC (H82A), GATATAATGGCCCAAGATGAAGAAC (H82L), GATATAATGGGCTATGATGAAG (G83S), CCTCATACTCTTTCTCTAAAGAC (K115E), CATATCCTCATACTTTTTTTTTAA (E117K), ACCACTATATATTTTTAGTAG (R163I), CTACCACTATACTTTTTTAGTAGTAC (R163K), CTCATTATCTGGGTAATAAAAATTA (W178Y), CGTCTCATTACTTGGCCAAT (D180S), CACTTTATATTTAGCTTGTAC (D198A), CACTTTATATTTTTCTTGTAC (D198E), CACTTTATATTTAGATTGTAC (D198S), GCTCACTTTAAATTTATCTTG (Y200F), GCTCACTTTAGATTTATCTTG (Y200S), ATTTATGTAGTTTTGAATTAC (D274N), ATTTATGTAGGATTGAATTAC (D274S). The selection primer and the H82A mutagenic primer were chemically 5′-phosphorylated during the syntheses and purified by gel electrophoresis. All other primers were phosphorylated with T4 polynucleotide kinase (New England Biolabs or Boehringer) and purified using Sephadex spin columns (Select-D G-25, 5 Prime 3 Prime, Inc.). Mutations were confirmed by sequencing the appropriate regions of the plasmids either using [^{35}S]dATP (Sequenase Version 2.0 DNA sequencing kit, Amersham) or nonradioactively using digoxygenin-labeled sequencing primers, a direct blotting procedure, and ELISA detection of DNA bands (GATC, Konstanz, Germany).

Purification of Wild-Type and Mutant PI-PLCs. Recombinant wild-type or mutant *B. cereus* PI-PLCs were expressed in *Escherichia coli* and isolated and purified as described (Ryan et al., 1996). Most mutants were further purified by gel filtration using HiLoad Superdex 75 prep grade (Pharmacia). Purified proteins were stored at −20 °C in 20 mM Tris-HCl, pH 8.5, 1 mM EDTA. The recombinant PI-PLCs were judged to be >95% pure by SDS−PAGE. The protein concentration of the preparations was determined by the absorbance at 280 nm where $E^{0.1\%} = 1.83$ for wild-type and mutant PI-PLCs except W178Y where $E^{0.1\%} = 1.73$.

Kinetic Evaluation of Wild-Type and Mutant PI-PLCs. The activity of mutant and wild-type PI-PLC toward detergent-solubilized PI was measured essentially as described previously (Griffith et al., 1991). Typically, a 10 mM suspension of tritiated PI was prepared by rehydrating a mixture of unlabeled and radiolabeled PI after organic solvent evaporation under vacuum. The specific radioactivity of the PI was about 80 000 cpm/mol. For the assay, 20 μL of the [^{3}H]PI suspension, 20 μL of 0.8% DOC, and 40 μL of 100 mM HEPES, 1 mM EDTA, pH 7.2, were combined in an Eppendorf tube and vortexed to form mixed micelles. Reactions were initiated by the addition of *B. cereus* PI-PLC in 20 μL of 0.1% BSA, 20 mM HEPES, and 1 mM EDTA, pH 7.2, to give a final volume of 100 μL. Prior to addition, enzyme had been diluted in the same buffer and was kept on ice. Reactions were vortexed briefly and incubated at 37 °C for 10−40 min. Reaction blanks were included and contained 20 μL of 0.1% BSA, 20 mM HEPES, and 1 mM EDTA, pH 7.2, in place of enzyme. The pH of the buffers had been adjusted at 25 °C and will drop to about pH 7 at the incubation temperature of 37 °C. Assays were terminated by the addition of 0.5 mL of chloroform/methanol/HCl (66:33:1, by volume) with vortex mixing. The phases were separated by centrifugation, and water-soluble products were determined by scintillation counting of an aliquot of the upper aqueous phase. Conditions of linearity of enzymatic activity with time were met by assuring that the reactions were terminated when no more than 10% of substrate had been turned into product. For wild-type PI-PLC, linearity was observed for at least 40 min in the presence of about 1.8 ng/mL (54 pM) enzyme. Up to 105-fold higher protein concentrations were used to detect residual activities in mutant PI-PLC enzymes. In this case, the enzyme had been transferred from its storage buffer to 20 mM HEPES, 1 mM EDTA, pH 7.2, using a Microcon-30 (Amicon) concentrator. After determining the protein concentration, BSA was added to 0.1%.

For the assay of PI-PLC activity using the synthetic substrate *myo*-inositol 1-(4-nitrophenyl phosphate) (NPIP),

racemic NPIP was synthesized using published procedures (Shashidhar et al., 1991). Aqueous stock solutions of NPIP were prepared, characterized, and stored as described (Ryan et al., 1996). Substrate concentrations given refer to the D-enantiomer only; the L-enantiomer was shown to be neither a substrate nor an inhibitor for PI-PLC (Leigh et al., 1992). The rate of substrate hydrolysis by PI-PLC was measured in 0.5 mL or 0.6 mL reactions containing 0.25 mM NPIP that were thermostated at 25 °C. The composition of the assay and measurement of enzyme-catalyzed NPIP hydrolysis were as described (Ryan et al., 1996).

For a 0.5 mL reaction volume, 360 μL of 1.25× assay buffer (125 mM HEPES, 1.25 mM EDTA, pH 7.0), 40 μL of 0.1% PEG-8000 in 1.25× assay buffer, and H_2O to 492.5 μL were combined in a disposable methacrylate semi-micro cuvette. A few minutes before the reaction was started 2.5 μL of 50 mM NPIP was added and mixed. The reaction was initiated by adding 5 μL of diluted enzyme and mixing immediately by rapid inversion. Enzyme dilutions were prepared in 0.1% PEG-8000, 6 mM HEPES, and 0.06 mM EDTA, pH 7.0.

The progress of NPIP hydrolysis was followed by monitoring the accumulation of the *p*-nitrophenolate (pNP) anion hydrolysis product for at least 4 min commencing within 15 s after addition of enzyme. Low-activity mutants were monitored for up to 90 min. Spectrophotometric detection of pNP product was at 399 nm (Beckman DU-40 spectrophotometer) or 405 nm (Eppendorf PR2210 spectrophotometer). The molar extinction coefficient of pNP was determined for the reaction conditions and the two wavelengths used. To obtain the initial velocity of the reaction, the progress curve was fitted by nonlinear regression to a first-order rate equation using GraFit Version 3.0 (Erithacus Software, Ltd., Staines, U.K.). Alternatively, initial rates were derived manually from the linear portion of the progress curve. Only data points below 0.8 AU, the region of linear response of pNP concentration vs absorbance, were used, and results obtained by either method are comparable.

Assay results are presented as the mean of at least two experiments. Values of repeat experiments may deviate by up to 20%. Factors leading to these variations include (I) the recombinant enzyme was purified from different isolates of the same transformant, (II) independent dilutions of the same enzyme preparation were used in repeat measurements, (III) different preparations of substrate were used, and (IV) assays were performed at different periods of time after purification of the enzyme. Under the conditions described, the specific activity for the turnover of 2 mM PI by wild-type PI-PLC was 2200 mol min^{-1} mg^{-1}, and the specific activity for the cleavage of 0.25 mM NPIP was 29 mol min^{-1} mg^{-1}. Approximate kinetic parameters of $K_M = 5$ mM and $V_{max} = 650$ mol min^{-1} mg^{-1} for the hydrolysis of D-NPIP by *B. cereus* PI-PLC have been determined previously (Leigh et al., 1992). Assays using either NPIP or PI were performed at substrate concentrations that exceeded enzyme concentrations by a factor between 80 for mutants with the lowest activities (i.e., H32A in the PI assay and R69K in the NPIP assay) and 105 or 107 for wild-type PI-PLC using the NPIP or PI assays, respectively.

For the turnover of PI, the determination of kinetic parameters is more complex as they are subject to the aggregate form of the substrate. A $K_{M\ app}$ of 1.4 mM has been reported for assay conditions that include the same concentration of DOC as used here but done at 25 °C and pH 7.5 (Ikezawa et al., 1976).

Crystallization and Data Collection. Crystallization of a number of *B. cereus* PI-PLC mutants was performed by hanging-drop vapor diffusion at 4 and 20 °C using similar crystallization conditions as described before for wild-type PI-PLC (Bullock et al., 1993; Heinz et al., 1995). Droplets were prepared by mixing 5 μL of the premixed protein solution (10 mg/mL protein, 20 mM HEPES, pH 7.9, and 0.01% NaN_3) and 5 μL of precipitant solution (36% PEG 600, 0.2 M trisodium citrate, and 20 mM HEPES, pH 7.9). To increase crystal size 1 μL of 1 mM $CdCl_2$ solution was added to some droplets (Trakhanov & Quiocho, 1995). The drop was placed over a reservoir containing 0.5 mL of 1.5−2.25 M NaCl. Crystals suitable in size for data collection were obtained after 2−6 weeks. Prior to mounting of the crystals, the drop was diluted using precipitant solution.

Structure Determination and Refinement. X-ray data were collected from single crystals of six different mutants to maximum resolutions between 2.0 and 2.7 Å on a Siemens X1000 area detector using graphite-monochromated CuK radiation from a Rigaku RU-200BH rotating-anode X-ray generator. Data were subsequently processed using the program XDS (Kabsch, 1988). Data collection statistics are summarized in Table 1. After rigid-body refinement against the new data using the program X-PLOR 3.851 (Brünger et al., 1989), an $F_o - F_c$ electron density map was computed using all reflections and the 2.6 Å structure of PI-PLC (Heinz et al., 1995) for phasing. After visual inspection of the map using the program O 5.9 (Jones et al., 1991), the respective mutation was manually introduced in the model. For mutant D274N that crystallized nonisomorphously in the presence of $CdCl_2$ at 20 °C, the structure was determined by molecular replacement using the program AMoRe (Navaza, 1994) and the coordinates of wild-type PI-PLC as a search model.

Subsequently the models were subjected to several cycles of simulated annealing and positional and restrained *B*-factor refinement using the program XPLOR 3.851 interrupted by manual corrections. Solvent molecules were gradually incorporated into the structure using the automatic water-fitting procedure in the program AWAT (Meyer, 1997) and a cutoff of $>+3$ in $F_o - F_c$ maps. Solvent molecules were kept in the structure if at least one hydrogen bonding partner was available and the *B*-factors were below 70 $Å^2$. The qualities of the final models were assessed using the programs PROCHECK (Morris et al., 1992) and WHATCHECK (Vriend & Sander, 1993). In the Ramachandran plot (Morris et al., 1992), between 82 and 87% of all residues were located in the most favored regions and no non-glycine residue in the disallowed regions. Refinement statistics are summarized in Table 1. The coordinates of the PI-PLC mutants were deposited with the Protein Data Bank (PDB entry codes: 2ptd, 3ptd, 4ptd, 5ptd, 6ptd, and 7ptd; Bernstein et al., 1977).

Structural Superpositions. Superpositions of mutant and wild-type PI-PLCs were performed using the program LSQMAN (Jones et al., 1991). Superpositions of the triad present in the complex between PI-PLC and *myo*-inositol with the catalytic triads in α-chymotrypsin (1.7 Å resolution, PDB entry code 4cha), subtilisin BPN' (2.2 Å resolution, 5sic), and lipase from *Geotrichum candidum* (1.8 Å resolution, 1thg) were performed in a pairwise manner by using the lsq _explicit option of the program LSQMAN (Jones et

Table 1: X-ray Data Collection and Refinement Statistics

parameters	H32A	H32L	R163K	D198E	D274N	D274S
			Data Collection			
space group	$P2_12_12_1$	$P2_12_12_1$	$P2_12_12_1$	$P2_12_12_1$	$P2_12_12_1$	$P2_12_12_1$
cell constants *a*, *b*, *c* (Å)	45.1, 46.2, 160.5	45.2, 46.0, 161.2	45.2, 46.0, 161.0	45.6, 45.9, 161.7	44.7, 44.6, 153.3	45.2, 46.1, 161.0
R_{merge} (%)[a]	10.7	5.7	7.3	4.7	5.3	4.2
no. of observations	26905	21263	17915	38556	21317	35135
no. of unique reflections	9252	9104	9137	18406	12218	16336
completeness (%)	84.7 (59.9)[b]	84.1 (54.8)	76.3 (26.2)	79.9 (40.1)	86.6 (71.3)	71.2 (43.3)
resolution range (Å)	40.1−2.6	18.9−2.6	18.7−2.5	19.7−2.0	6.3−2.3	19.7−2.0
I/σ_I	6.6 (1.9)[b]	12.8 (5.3)	9.9 (3.7)	14.6 (5.4)	12.0 (3.6)	14.3 (4.6)
			Refinement			
resolution range (Å)	20−2.7	18.9−2.6	18.7−2.6	19.7−2.0	6.3−2.3	19.7−2.2
no. of non-H protein atoms	2417	2420	2420	2423	2422	2420
number of solvent molecules	118	86	89	126	60	122
no. of reflections ($F > 0$)	8082	9104	8862	18406	12216	12181
R-factor (%)[c]	17.9	18.2	18.7	19.8	20.3	17.7
R_{free} (%)[d]	29.2	29.4	32.4	27.1	27.0	26.2
$\Delta_{\text{bond lengths}}$ (Å)[e]	0.006	0.007	0.007	0.007	0.007	0.006
$\Delta_{\text{bond angles}}$ (deg)[e]	1.35	1.33	1.29	1.4	1.4	1.35

[a] $R_{sym} = \sum_{hkl}\sum_i|I_{(hkl,i)} - \langle I_{(hkl)}\rangle|/\sum_{hkl}\sum_i\langle I_{(hkl)}\rangle$, where $I_{(hkl,i)}$ is the scaled intensity of the *i*th measurement and $\langle I_{(hkl)}\rangle$ is the mean intensity for that reflection. [b] Statistics for data in the highest resolution shell are given in parentheses. [c] *R*-factor $= \sum||F_o| - |F_c|/\sum|F_o|$, where $|F_o|$ and $|F_c|$ are the observed and calculated structure factor amplitudes, respectively. [d] (5% of the data omitted prior to refinement (Brünger, 1992). [e] $\Delta_{\text{bond lengths}}$, $\Delta_{\text{bond angles}}$ give the average discrepancy between these parameters in the refined structure and their "ideal" values.

al., 1991) which is based on a simple least-squares fit of two atom lists containing three atoms. For PI-PLC, this list contained atoms 2-OH of inositol, $N^{\epsilon 2}$ of His32, and $O^{\delta 2}$ of Asp274; for α-chymotrypsin, atoms O^{γ} of Ser195, $N^{\epsilon 2}$ of His57, and $O^{\delta 1}$ of Asp102; for subtilisin, atoms O^{γ} of Ser221, $N^{\epsilon 2}$ of His64, and $O^{\delta 1}$ of Asp32; for lipase, atoms O^{γ} of Ser217, atom $N^{\epsilon 2}$ of His463, and $O^{\epsilon 2}$ of Glu354.

For the spatial comparison of the catalytic histidines in PI-PLC (His32 and His82) and RNase A (His12 and His119), the imidazole groups of the analogous histidines were superimposed by hand.

scyllo, *epi*, D-*chiro*, and L-*chiro* stereoisomers of inositol were generated from *myo*-inositol measurements that have been determined for the crystal structure of the PI-PLC in complex with *myo*-inositol (PDB entry code 1ptg; Heinz et al., 1995) by moving individual OH groups from axial to equatorial positions or *vice versa*. After local energy minimization, the six ring carbon atoms were used to superimpose the individual structures onto *myo*-inositol located at the active site of PI-PLC (CS Chem3D Pro Vs. 3.5, Cambridge Soft Corp.).

RESULTS

Mutant Design and Active Site Geometry. The crystal structure of *B. cereus* PI-PLC in complex with *myo*-inositol identified those amino acids most likely to be involved in binding the substrate head group and in catalysis (Heinz et al., 1995). The structure shows *myo*-inositol binding in an edge-on mode to the active site and forming a number of specific interactions with amino acid side chains (Figure 3). These comprise hydrogen bonding interactions between the side chains of His32, Arg69, Arg163, and Asp198 and the inositol hydroxyls in positions 2, 3, 4, and 5 as well as a hydrophobic coplanar stacking interaction with the aromatic side chain of Tyr200. Both His32 and Arg69 were proposed to play an essential role in catalysis: His32 as the general base to activate the 2-OH group of PI and Arg69 to stabilize the negatively charged pentacovalent transition state (Heinz et al., 1995). In the proposed catalytic mechanism, His82 acts as a general acid. Both His32 and His82 are conserved in all PI-PLCs. To investigate the importance of these amino acids in substrate binding and catalysis, the following set of mutants carrying conservative as well as nonconservative replacements was constructed: H32A, H32L, R69A, R69E, R69K, H82A, H82L, R163K, R163I, D198A, D198E, D198S, Y200F, and Y200S. In the structure of PI-PLC, the side chains of the residues listed above are spatially correctly oriented, even in the absence of *myo*-inositol, via a hydrogen bonding network with a number of "supporting" amino acids (Figure 3). These do not directly interact with the inositol and include Lys115, Glu117, Trp178, Asp180, and Asp274. Due to its interaction with His32, Asp274 was proposed to be a member of a triad consisting of Asp274, His32, and the 2-OH group of the inositol head group of the substrate (Heinz et al., 1995). Mutants K115E, E117K, W178Y, and D180S were constructed to disrupt the hydrogen bonding interactions. In addition, mutants D274N and D274S were made to verify the active role of Asp274 in catalysis.

In addition to the two catalytic histidines, Gly83 is also highly conserved in PI-PLCs. In the PI-PLC structure, Gly83 is located in a loop and assumes main chain dihedral angles ($\phi = 79°$, $\psi = -116°$) that are only allowed for glycine residues. Gly83 is located adjacent to His82, suggesting a role of Gly83 in correctly positioning His82 for catalysis. Its small hydrogen atom side chain also points into the active site pocket. Mutant G83S was constructed to change its main chain geometry and to see whether this change was transmitted to His82, possibly causing a decrease in catalytic activity.

Most of the amino acids targeted for mutagenesis are also conserved in the PI-PLCs from *S. aureus* (Daugherty & Low, 1993) and *L. monocytogenes* (except for Arg163, Trp 178, and Asp180; Leimeister-Wächter et al., 1991).

Crystal Structures of Mutant PI-PLCs. Crystals suitable for data collection were obtained of the following mutants: H32A, H32L, R163K, D198E, D274N, and D274S. The crystal structures of these mutants were determined by difference Fourier techniques (except D274N) and refined at a resolution between 2.0 Å (D198E) and 2.7 Å (H32A) (Table 1). The initial difference Fourier maps with coefficients $F_{mutant} - F_{WT}$, α_{WT} (where F_{mutant} and F_{WT} designate

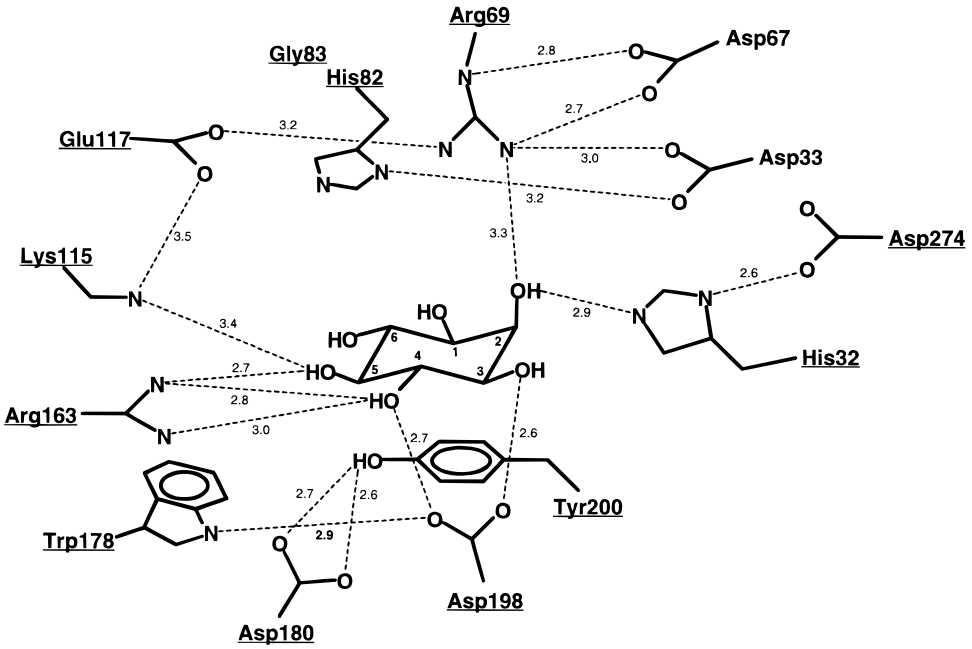

FIGURE 3: Schematic drawing of the active site of *B. cereus* PI-PLC in complex with the inhibitor *myo*-inositol (center). Besides residues directly interacting with inositol, residues participating in the extensive hydrogen bonding network are also shown. For simplicity, in most cases only the functional head groups of the side chains are shown. Interatomic distances (in Å) are indicated by dotted lines. The names of amino acids that were mutated in this study are underlined.

the structure amplitudes of mutant and wild-type crystals, respectively, and α_{WT} the phase angles calculated from the wild-type structure) calculated after rigid-body refinement showed as largest features the site of mutation that was clearly interpretable. With the exception of positive peaks accounting for solvent molecules, the rest of the map was essentially featureless.

Mutant D274N was crystallized at 20 °C in the presence of 1 mM $CdCl_2$. Despite a similar habitus when compared with wild-type PI-PLC crystals, space group determination revealed slightly shortened *a*- and *b*-axes and a decrease of the *c*-axis of almost 10%, indicating nonisomorphism. Structure determination of mutant D274N by molecular replacement was straightforward with a correlation of 0.81 and an *R*-factor of 29.1%. Globally, the crystal packing was preserved with only slight shifts along common interfaces, with the exception of the crystal contact between molecules related by the symmetry operator $-x, y+1/2, -z+1/2$, where larger shifts were observed. The site of mutation was not involved in crystal contacts and did not show any visible changes accordingly. Crystals of D274N grown in the presence of 1 mM $CdCl_2$ at 4 °C showed a gradual conversion of a wild-type-like packing to the new packing during data collection at 20 °C (unpublished experiments). The observed connection between the presence of $CdCl_2$ and a temperature change from 4 to 20 °C in PI-PLC crystals will be the subject of further investigation.

R-factors for the mutants prior to combined positional and *B*-factor refinement were between 22 and 24%. After refinement, the PI-PLC mutant structures were very similar to wild-type PI-PLC with a root-mean-square (rms) deviation for all C_α atoms in the range of 0.3−0.4 Å. Superpositions of the active sites in mutant and wild-type structures resulted in rms deviations of 0.3 Å. These values are within the estimated positional error (0.25−0.35 Å).

His32→Ala, Leu. The site of mutation showed the expected loss of the imidazole group of His32 but essentially no changes for other residues even in the close vicinity of the mutation. When *myo*-inositol was modeled into the active site of mutant H32A, all wild-type interactions (Figure 4a) except for the critical hydrogen bond between His32 and the 2-OH group of inositol were preserved (Figure 4b). In mutant H32L, the newly introduced leucine side chain filled part of the former position of the histidine and, as expected, did not productively interact with neighboring side chains or a modeled *myo*-inositol molecule (Figure 4c). In both mutants, the side chain of Asp274 that forms a hydrogen bond with His32 in the wild-type enzyme remained unchanged as well.

Arg163→Lys. The conservative replacement of Arg163 with lysine caused no changes in the active site except for the site of mutation. The side-chain of Lys163 oriented in an extended conformation essentially following the path of the former arginine side chain and was still able to form a hydrogen bonding interaction with the 4-OH group of a modeled inositol molecule (Figure 4d).

Asp198→Glu. The conservative replacement of Asp198 with a glutamate caused more drastic changes in the active site. Because of its additional methylene group Glu198 was able to form salt-bridge-like interactions with Arg163 and Arg69 across the *myo*-inositol binding pocket while the hydrogen bonding interaction with the side chain of Trp178 was maintained (Figure 4e). The close interactions between Glu198 and Arg163 and Arg69 were made possible by a concerted 0.5 Å movement of main chain segments 67−72, 115−118, and 163−165 toward the active site pocket and segments 173−176 and 184−186 away from the active site without affecting the side chain torsion angles of Arg69 and Arg163.

Asp274→Asn, Ser. The replacement of Asp274 by its isosteric counterpart, asparagine, caused no visible changes in the structure. Asn274 still forms a hydrogen bonding interaction via its $O^{\delta 1}$ atom with atom $N^{\delta 1}$ of His32 and is fully superimposable on the former position of Asp274. Due

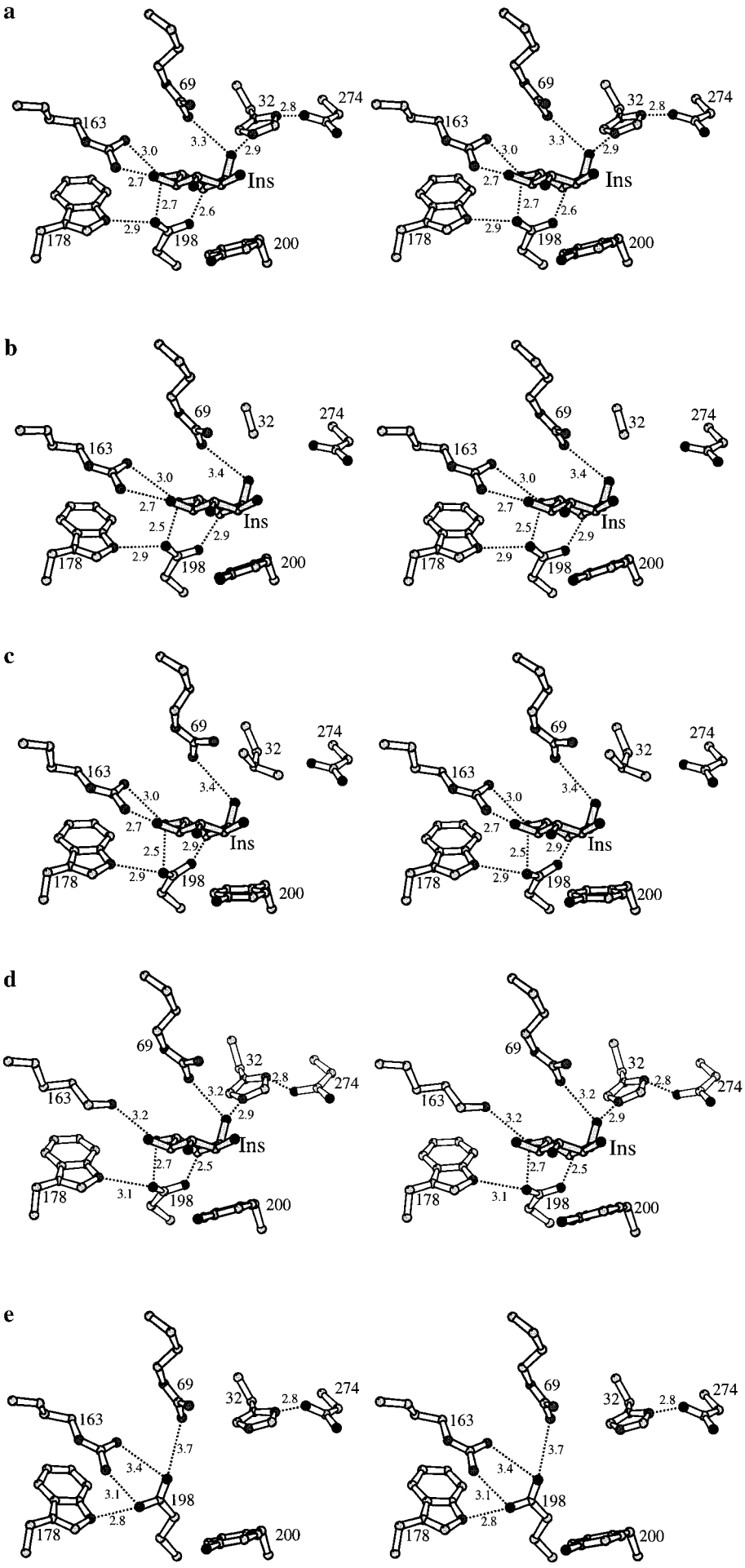
a
69
32
2.8
274
163
3.3
3.0
2.9
2.7
Ins
2.7
2.6
2.9
178
198
200
b
69
32
274
163
3.4
3.0
2.7
2.5
2.9
Ins
2.9
178
198
200
c
69
32
274
163
3.4
3.0
2.7
2.5
2.9
Ins
2.9
178
198
200
d
69
32
2.8
274
163
3.2
2.9
3.2
Ins
2.7
2.5
178
3.1
198
200
e
69
32
2.8
274
163
3.7
3.4
3.1
198
2.8
178
200

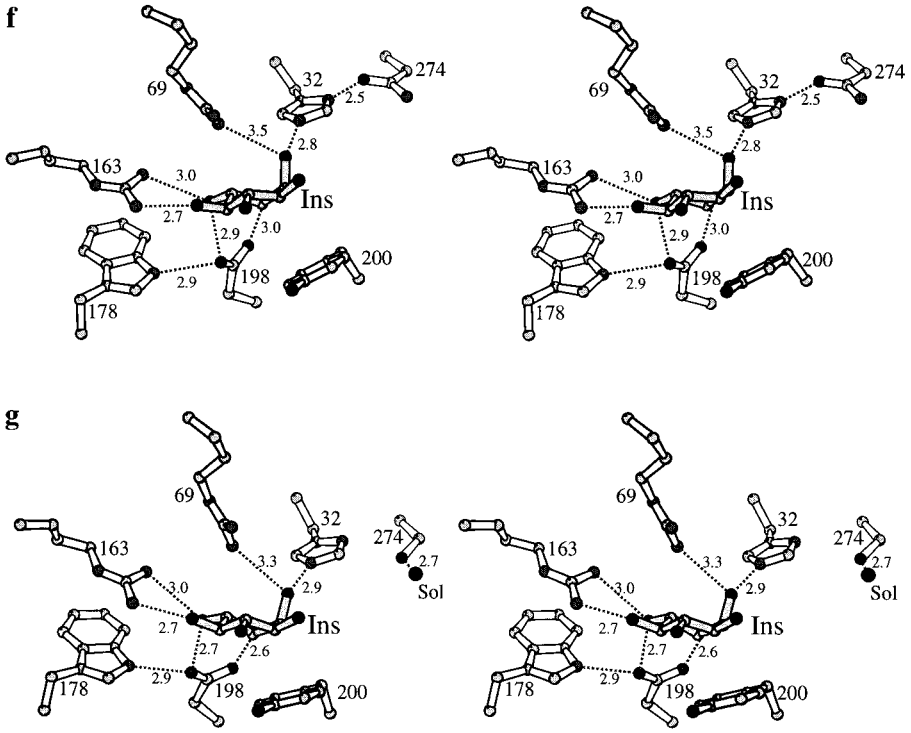

FIGURE 4: Stereo pictures showing the active sites of wild-type PI-PLC (panel a) and the mutants H32A (panel b), H32L (panel c), R163K (panel d), D198E (panel e), D274N (panel f), and D274S (panel g) in similar orientations. Carbon atoms are shown in light gray, nitrogen atoms in medium gray and oxygen atoms in black. Bound or modeled *myo*-inositol (see text) is shown with gray bonds and labeled Ins. For clarity, only the side chain atoms of residues in postions 32, 69, 163, 178, 198, 200, and 274 are selected. Hydrogen bonding interactions are shown as dotted lines (distances in Å).

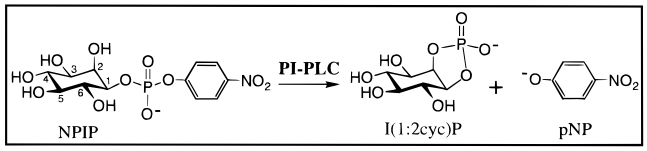

FIGURE 5: *p*-Nitrophenyl phosphoryl ester NPIP (colorless) is cleaved by *B. cereus* PI-PLC to form the highly colored nitrophenylate anion (pNP), which is monitored in a continuous spectrophotometric assay.

to the absence of any structural perturbations, a *myo*-inositol molecule could be easily modeled into the active site (Figure 4f). In mutant D274S, structural changes are restricted to the site of mutation. Ser274 adopts an ideal χ_1 angle of $-55°$ and forms no close interactions with His32 anymore but instead a hydrogen bonding interaction with a newly introduced solvent molecule (Figure 4g).

Enzyme Activity. Kinetic analysis of phospholipases is complicated by the fact that the natural substrate is insoluble in water in a monomeric form, and the enzymes exhibit surface activation when in contact with lipid aggregates (micelles or vesicles). We adopted a strategy of using two different assays to describe the catalytic activity of mutant enzymes more effectively. One assay utilizes ^{3}H-labeled PI solubilized in the detergent DOC. Despite the advantage of PI being the natural substrate, this assay is limited by the effect the detergent can have on enzyme activity, and for a detailed analysis, the equilibrium distribution of enzyme between the aqueous phase and micelles must be taken into account for each mutant. The second assay utilizes the water-soluble synthetic substrate NPIP (Figure 5). Advantages of NPIP are that no detergent micelles or vesicles are required and this substrate permits a continuous spectrophotometric assay. A third advantage is that the leaving group is very different from that of the natural substrate, so that in certain cases additional information is available. The main limitation of NPIP is that the Michaelis constant, K_M, is about 1 order of magnitude higher than for PI, and very large amounts of this chromogenic reagent are required in order to obtain kinetic constants (Shashidhar et al., 1991; Leigh et al., 1992; Martin & Wagman, 1996). NPIP is not commercially available, and supplies were deemed too limited to carry out a complete kinetic analysis for the mutants. For these reasons, we focused on obtaining the relative catalytic activities for all mutants described above using both assays. The kinetic data are reported in Table 2.

All mutants showed a reduced activity when compared with the activity of the native enzyme with a good correlation in most cases for both substrates despite their different structures. An interesting exception is the His82L mutant where the PI activity is abolished, but about 13% of the NPIP activity remains. Essentially no activity was detected for mutants where His32, Arg69, and Asp198 were replaced. Likewise, the R163I and D274S mutants were inactive in both assays. The highest residual activities (up to about half of the wild type activity) were found for mutants D180S and Y200F.

The relative catalytic rates though not a direct measure of substrate binding are together with the structural data a good indicator that substrate binding and/or catalytic steps were altered in the mutant enzymes.

DISCUSSION

To obtain a correlation of the kinetic and structural data described in this study, PI-PLC mutants were divided into three groups according to the putative role of the target amino acid as derived from the crystal structure of PI-PLC in

Table 2: Catalytic Activity of Mutant *B. cereus* PI-PLCs[a]

mutant	NPIP assay (%)[b,c]	[^{3}H]PI assay (%)[b,c]
H32A	<0.004	0.0001
H32L	<0.003	0.0005
R69A	<0.7	<0.5
R69E	<0.7	<2.1
R69K	0.002	0.002
H82A	—[d]	<0.0007
H82L	12.5	0.007
G83S	2.5	8.4
K115E	24.8	—[d]
E117K	1.0	1.2
R163K	8.6	27.4
R163I	<0.7	2.0[e]
W178Y	6.5	15.3
D180S	57.0	34.0
D198A	<0.7	<0.9
D198E	<0.7	<0.6
D198S	<0.7	0.2
Y200F	43.2	48.8
Y200S	1.0	2.2[e]
D274N	15.2	4.2
D274S	<0.7	<0.9

[a] Enzyme activities were measured at pH 7 and 25 °C using 0.25 mM NPIP substrate or at 37 °C using 2 mM PI substrate. [b] The mean of two or more experiments is shown as the percent of wild-type activity. [c] When no activity was seen, this is expressed as activity smaller than the detection limit (1.5 × negative control). [d] Not determined. [e] Activity is estimated from consistent values at or below the detection limit.

complex with *myo*-inositol: residues directly involved in catalysis, residues involved in binding to the head group of PI, and residues that are not directly involved in catalysis and substrate binding but might play a supportive role. Results for the first two groups are also viewed in context of possible binding to the active site of different inositol stereoisomers some of which occur naturally in phospholipids.

Mutations of Residues Involved in Catalysis: Amino Acid Positions 32, 69, 82, and 274. Because of their strict conservation and their location in the active site of *B. cereus* PI-PLC (Heinz et al., 1995), both His32 and His82 were proposed to act as a general base and acid, respectively, in analogy to RNase A (Richards & Wyckhoff, 1971). The replacement of the His32 with either alanine or leucine resulted in a complete loss of activity in both assays. The crystal structures of both mutants showed essentially no changes in the structure beyond the site of mutation (Figure 4b,c). Even though the hydrogen bonding potential of the 2-OH group of inositol is satisfied by the interaction with the side chain of Arg69, these mutants have lost one hydrogen bonding interaction with *myo*-inositol which would reduce the enzyme's affinity for the substrate. In itself, this effect is not large enough to account for the complete loss of activity; rather the results are indicative of a direct involvement of His32 in catalysis. Two histidines, His311 and His356, are found in locations and orientations similar to His32 and His82, respectively, in the active site of mammalian PI-PLCδ_1 (Essen et al., 1996), and their critical role in catalysis has been confirmed by mutagenesis (Ellis et al., 1995; Cheng et al., 1995) although His311 might not act as the general base during catalysis (Essen et al., 1997).

There is an important difference between the relative activities of the His32 and His82 mutants in the two assays. Whereas the activity of the His32 mutants is completely abolished in both assays, the H82L mutant gives noticeably different results. With PI as the substrate, a complete loss of activity is observed, but activity toward NPIP is still about 13% of wild type. This observation is reminiscent of the behavior of RNase A. Thompson and Raines (1994) observed that when His12 (analogous to His32 of PI-PLC) was replaced with alanine, the activity of the mutant was abolished toward the oligo- or dinucleotide substrates poly(cytidylic acid) [poly(C)] and uridylyl(3′→5′)adenosine (UpA), as well as the chromogenic substrate uridine 3′-(*p*-nitrophenyl phosphate). When His119 (analogues to His82 of PI-PLC) was replaced with alanine, the activities toward the substrates poly(C) and UpA were again abolished. However, the activity with uridine 3′-(*p*-nitrophenyl phosphate), although reduced from the wild type, was by no means abolished. The explanation is that *p*-nitrophenoxy anion is a much better leaving group than an alkoxide anion, and does not require the assistance of His119. This provides direct evidence that the role of His119 is that of a general acid, i.e., to protonate the leaving group. Similarly, in the case of *B. cereus* PI-PLC, the residual activity of H82L with NPIP as the substrate provides the first direct evidence that His82 is the general acid in enzyme catalysis. In fact, the superposition of the catalytic histidines in PI-PLC and RNase showed a high positional agreement of the imidazole groups with very similar distances between both groups despite no structural homology between both enzymes (Figure 6).

Asp274 together with His32 are highly conserved in bacterial PI-PLCs, but Asp274 is replaced by an asparagine in the mammalian PI-PLCδ_1 (Essen et al., 1996). The side chain of Asp274 is partially buried with no direct access to the active site pocket. Asp274 forms a hydrogen bonding interaction with the side chain of the catalytic His32 which itself forms another hydrogen bond with the 2-OH group of *myo*-inositol (Figure 3). This structural ensemble of chemical groups closely resembles that found for the catalytic triads present in many hydrolases. A pairwise superposition of the catalytic triads of α-chymotrypsin, subtilisin BPN′, and lipase with the triad in the PI-PLC−*myo*-inositol complex gave an excellent agreement, with rms-deviations ranging from 0.36 to 0.7 Å (Figure 7). Residual activities of 15.2% toward NPIP and 1.2% toward [^{3}H]PI were found for mutant D274N. These were in the range reported for the analogous mutant D102N in trypsin (Corey & Craik, 1992). The crystal structure of D274N showed the position of Asn274 virtually unchanged when compared with Asp274 in wild-type PI-PLC, and Asn274 still forms a hydrogen bonding interaction with His32 (Figure 4f). Enzyme activity was abolished in mutant D274S where Ser274 no longer interacted with His32, which itself maintained its location (Figure 4g). These data demonstrate that Asp274 is a critical residue, supporting its proposed role as a member of the triad.

The replacement of Arg69 with alanine, glutamate, or lysine lead to a dramatic decrease of catalytic activity to less than 1%. The fact that this large decrease in activity is observed for different replacements underscores the critical role of Arg69 in catalysis. Arg69 weakly interacts with the 2-OH group of *myo*-inositol, but due to the relatively long distance of 3.3 Å of this interaction, Arg69 would only make a minor contribution to substrate binding. Taken together, these observations argue that the role of the positively charged Arg69 is to stabilize the negatively charged pentacovalent transition state during the catalytic reaction. In addition, in the crystal structure of the mammalian PI-PLCδ_1,

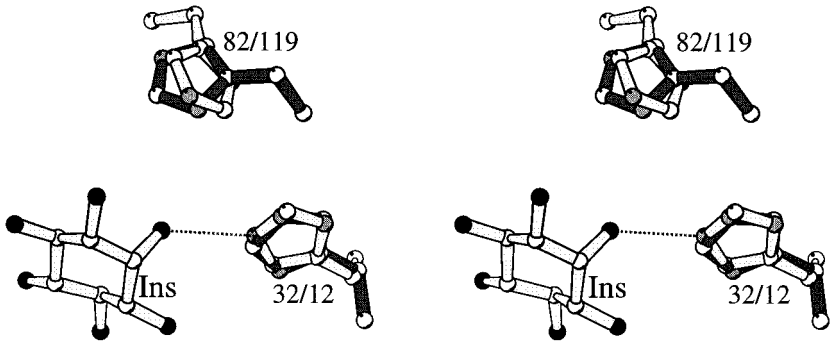

FIGURE 6: Stereo picture showing the side chains of His32 and His82 as well as *myo*-inositol (Ins) located in the active site of PI-PLC (light gray bonds). Superimposed are the side chains of the analogous catalytic histidines in ribonuclease A, His12 and His119 (dark gray bonds).

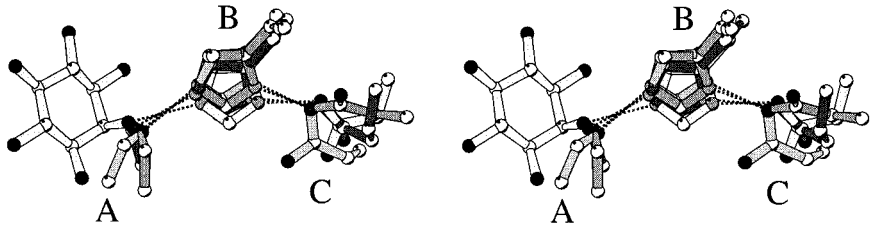

FIGURE 7: Stereo picture showing a superposition of the catalytic triads of PI-PLC, α-chymotrypsin, subtilisin, and lipase (see text). Hydrogen bonding distances are indicated by dotted lines. The three parts of the triads are labeled A [serine or inositol (in the case of PI-PLC)], B (His), and C [Asp or Glu (in the case of lipase)].

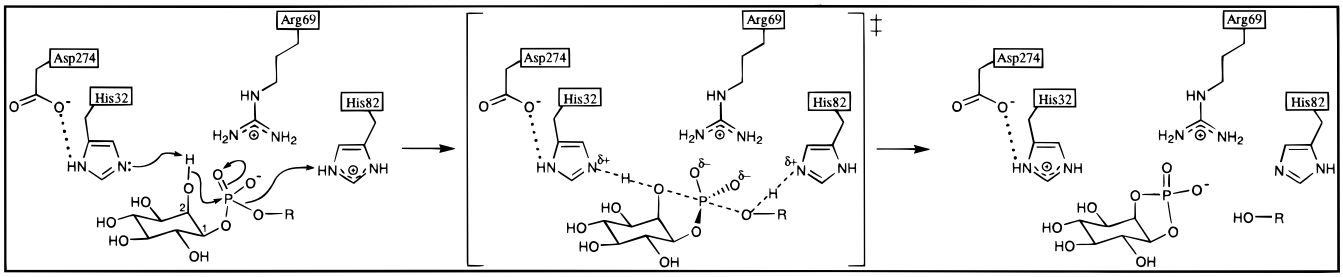

FIGURE 8: Proposed catalytic mechanism of *B. cereus* PI-PLC. Four residues play a critical role in catalysis, His32, His82, Arg69, and Asp274, as established by site-directed mutagenesis. The imidazole ring of His32 acts as a base, accepting a proton from the 2-OH group of *myo*-inositol and facilitating the nucleophilic attack of this oxygen atom on phosphorous to form a pentacovalent transition state. At the same time, the protonated imidazole ring of His82 acts as an acid, donating its proton to the *sn*-3 oxygen of PI, weakening this oxygen−phosphorus bond, and eventually producing a good leaving group, diacylglycerol (HO−R). The positively charged Arg69 stabilizes the negatively charged pentacovalent transition state. The *myo*-inositol 1,2-cyclic phosphate product of this phosphotransferase reaction can then act as a substrate in the second reaction, a slow hydrolysis to produce D-*myo*-inositol 1-phosphate. The mechanism of the second reaction is essentially the reverse of that shown above, but with water substituting for HO−R, and producing D-*myo*-inositol 1-phosphate.

Arg69 is replaced by a glutamate that is one of the ligands for a Ca^{2+} ion essential for catalysis (Essen et al., 1996). The Ca^{2+} at the active site has been proposed to stabilize the transition state (Essen et al., 1997). The Ca^{2+} ion exactly overlays on top of the guanidinium head group of Arg69 in *B. cereus* PI-PLC, suggesting a similar role for Arg69. Replacement of Arg69 with glutamate would certainly disrupt the intricate hydrogen bonding network between the side chains of Asp33 and Glu117 and Arg69 (Figure 3). The conservative replacement with lysine leads to a shortening of the side chain and may be accompanied by a weakening of the interactions with substrate or a reorientation of the lysine side chain away from the substrate.

These observations are summarized in the catalytic mechanism shown in Figure 8. This enzymatically mediated general acid−base catalysis is consistent with all available information on this enzyme (see the introduction). More complex mechanisms, such as the addition of a phosphorane intermediate, as has been proposed as a modification of the simple acid−base catalysis in ribonuclease A (Breslow & Chapman, 1994), are not ruled out.

Mutation of Residues Involved in Substrate Binding: Amino Acid Positions 163, 198, and 200. Arg163 contributes to the binding of the inositol head group of PI by forming two hydrogen bonds with the 4-OH and 5-OH groups of inositol. The replacement of Arg163 with lysine resulted in a moderate reduction in catalytic activity (27.4% for [^{3}H]-PI; 8.6% for NPIP). In the crystal structure of mutant R163K, Lys163 is still able to contribute a single hydrogen bond to the 4-OH group of the modeled inositol (Figure 4d). The side chain of Lys163 is not involved in other polar interactions with the enzyme. Therefore, the observed reduction of activity is due to the loss of a single hydrogen bond between mutant enzyme and substrate. Not surprisingly, the substitution of Arg163 by a hydrophobic isoleucine resulted in an almost complete loss of activity. This is due to the loss of both hydrogen bonds between wild-type enzyme and substrate as well as the formation of a hydrophobic patch in the highly polar active site pocket that further disfavors the binding of the polar substrate.

Like Arg163, Asp198 also contributes to the binding of *myo*-inositol via two hydrogen bonding interactions. Mutations of Asp198 showed dramatic reductions in activity. Surprisingly, even the conservative replacement of Asp198 by glutamate resulted in an almost complete loss in activity. Glu198 would certainly maintain the hydrogen bonding potential of an aspartate. The crystal structure of this mutant showed the formation of new specific interactions of Glu198 with Arg163 and Arg69 across the inositol binding pocket (Figure 4e). These interactions will certainly prevent access of substrate to the active site. The mutations of Asp198 to alanine or serine lead to the loss of two hydrogen bonds to the inositol causing a similar loss in activity as observed for mutant R163I.

The phenol ring of Tyr200 is involved in a coplanar stacking interaction with the large apolar side of the inositol ring and forms a wall of the active site. With its free OH group, a hydrogen bonding interaction with Asp180 is formed. The conservative replacement of Tyr200 with phenylalanine resulted in a 50% reduction of activity. Phe200 is probably still able to form the stacking interaction, but due to the loss of the interaction with Asp180, a larger flexibility of the side chain of Phe200 in the active site might interfere with substrate binding. The importance of Tyr200 in forming part of the head-group binding pocket is exemplified by the observation that mutant Y200S shows an activity of less than 1%.

Mutation of Residues Not Directly Involved in Substrate Binding or Catalysis: *Amino Acid Positions 83, 115, 117, 178, and 180.* Along with His82, Gly83 is strongly conserved in all known PI-PLCs. It is located in the elongated loop connecting β-strand 2 with helix 4. Because of its main chain torsion angles that are only allowed for glycine, it was proposed that Gly83 places the neighboring His82 at an optimal position for catalysis. The replacement of Gly83 with serine, which has less freedom in adopting its main chain torsion angles for steric reasons, lead to a moderate decrease in activity (2.5% for NPIP or 8.4% for [^{3}H]PI). The decrease of activity corroborates the proposed role of Gly83 as supportive for an optimal orientation of His82.

Lys115 interacts weakly with Glu117 as well as with the 5-OH group of inositol in wild-type PI-PLC. Mutation to glutamate results in a residual activity of 24.8%. This relatively high value indicates that Lys115 plays only a minor role in stabilizing the active site of PI-PLC. In contrast, mutation of Glu117, which is participating in a charged hydrogen bonding network that surrounds the active site and includes Arg69 and Asp33 (Figure 3), leads to a more profound reduction of activity to 1%. This could indicate that Lys117 in mutant E117K interferes with the likewise positively charged side chain of Arg69, which has been shown to be very position-sensitive with respect to stabilizing the negatively charged transition state in an optimal way during catalysis (see above).

Trp178 fulfills a dual function in PI-PLC by separating the bottom of the active site from the core of the protein and by forming a hydrogen bond with the side chain of Asp198, a residue shown to be critical for substrate binding (see above). The conservative replacement of Trp178 by tyrosine eliminates the hydrogen bonding potential between positions 178 and 198. The observed decrease in activity to 6.5% for NPIP or 15.3% for [^{3}H]PI hydrolysis shows that Trp178 actively contributes to a stabilization of the active site.

The side chain of Asp180 forms a hydrogen bond to the side chain of Tyr200 that might contribute to a spatial fastening of Tyr200 which forms the side wall of the inositol binding pocket. The mutation of Asp180 to serine interrupts this interaction. The mutation is analogous to that introduced in Y200F which is reflected by a very similar moderate decrease in activity for mutant D180S to 57.0% (43.2% for Y200F) for the hydrolysis of NPIP and 34.0% (48.8% for Y200F) for [^{3}H]PI hydrolysis. These data show that the hydrogen bond between Asp180 and Tyr200 is not critical for optimal substrate binding and catalysis. This is corroborated by the fact that an aspartate equivalent to Asp180 is missing in PI-PLC from *L. monocytogenes* (Leimeister-Wächter et al., 1991).

Interactions of Stereoisomers of Inositol at the Active Site. The main theme of this work is the examination of the structure and function correlation at the active site of PI-PLC using mutagenesis of amino acid residues that contact the *myo*-inositol moiety of the substrate. With this information available, it is of interest to ask whether it is possible to account for data on inhibitors and substrates in which the stereochemistry of the inositol head group has been altered. A full analysis would require more information than is presently available, for example, a detailed knowledge of the phosphate and glycerol binding sites. Nevertheless, the stereochemistry of inositol itself provides some interesting clues, since substrate recognition is accomplished entirely through interactions with the inositol head group. Of the possible stereoisomers of inositol, some data on inhibitors or substrates containing *scyllo*-, D- and L-*chiro*-, and *epi*-isomers are available. For this reason, we have superimposed models of these isomers onto *myo*-inositol at the active site of *B. cereus* PI-PLC. *scyllo*-Inositol, which is derived from *myo*-inositol by setting the single axial OH group equatorial, is a symmetric molecule. Comparing the structures of the *myo*- and *scyllo*-isomers at the active site, the principal change we observe is the loss of the hydrogen bond to the catalytic His32. This is consistent with the 40-fold weaker inhibition reported for *scyllo*-inositol compared to *myo*-inositol (Ryan et al., 1996). A similar trend is seen in the corresponding short-chain phospholipids (Ryan et al., 1996; Martin & Wagman, 1996).

epi-Inositol differs from *myo*-inositol only by the presence of a second axial OH group. Maintaining the important axial 2-OH group, *epi*-inositol can be superimposed onto *myo*-inositol in two orientations: with axial OH groups at the C2 and C4 or C2 and C6 positions (retaining here, and in the description of other inositol isomers, the numbering system for *myo*-inositol; see Figure 1). We predict the orientation with axial OH groups at C2 and C4 should not bind to the enzyme as at least two of the three H-bonds to Asp198 and Arg163 can not form plus there would be a steric interference between 4-OH and Arg69. However, *epi*-inositol modeled into the active site in the second orientation, with axial OH groups at the C2 and C6 positions, maintains all H-bond interactions of *myo*-inositol and gains an additional interaction between 6-OH and Arg69 and possibly Lys115. This would explain the 5-fold increased inhibition observed for *epi*-inositol over *myo*-inositol (Ryan et al., 1996). The pro-chiral 1L-*myo*-inositol configuration (as in

L-*myo*-inositol 1-phosphate) also has an axial 6-OH group but lacks the axial 2-OH. Lack of the axial 2-OH explains that compounds bearing this head group cannot be substrates for PI-PLC as there is no nucleophile in a position to allow the formation of the transition state. However, in addition to not being substrates, 1L-*myo*-inositol phosphodiester derivatives apparently do not noticeably bind to the enzyme (Leigh et al., 1992; Lewis et al., 1993; Bruzik & Tsai, 1994). The lack of significant binding can be explained by of the lack of H-bonding to His32 via the 2-OH group and the presence of an H-bond between Arg69 and the axial 6-OH group. Engagement of Arg69 in H-bonds could obstruct its proper orientation around the 1-phosphoryl group at the 1 position.

L-*chiro*-Inositol was transposed into the active site of *B. cereus* PI-PLC in an orientation that corresponds to a 1L-*chiro*-inositol phospholipid substrate. In this orientation, the axial hydroxyl groups are located in the C2 and C3 positions. This arrangement differs from the 1D-*myo*-inositol group of the normal substrate only by a switch from equatorial to axial at the C3 position. This change brings Asp198 and the 3-OH closer together and also positions the 3-OH close to ring atom $C^{\delta 1}$ of Tyr200, interfering with the hydrophobic ring stacking. As a simple explanation, we may imagine that flexibility in the inositol ring and also in the side chain orientation of Asp198 allows 1L-*chiro*-PI to be a substrate, albeit at a turnover rate 103 times below that of the natural substrate 1D-*myo*-PI (Bruzik et al., 1994).

In summary, in this systematic study we succeeded in mapping the relative contribution of individual amino acids to catalysis. The data show the extraordinary sensitivity of the active site of PI-PLC toward mutations exemplified by the fact that even minor perturbations lead to a dramatic reduction of activity toward the natural substrate PI without causing major structural rearrangements. A comparison of enzyme activities of mutants for two different substrates provides the first direct biochemical evidence that His82 is acting as the acid in the catalytic mechanism. Furthermore, these results also explain the observed exquisite substrate head-group and inhibitor stereospecificity of PI-PLC that are preserved by an intricate hydrogen bonding network and a relatively rigid active site.

ACKNOWLEDGMENT

We thank Professor Georg E. Schulz for his generous support and for making his X-ray facilities available and Dr. Joachim Meyer for his assistance in X-ray data collection and processing. We are also grateful to Markus Krömer for his help with the molecular replacement method and Malik Lutzmann for producing a mutant.

REFERENCES

Bernstein, F. C., Koetzle, T., Williams, G., Meyer, E., Jr., Brice, M., Rodgers, J., Kennard, O., Shimanouchi, T., & Tasumi, M. (1977) *J. Mol. Biol. 112*, 535−542.
Berridge, M. J. (1993) *Nature 361*, 315−325.
Berridge, M. J., & Irvine, R. F. (1989) *Nature 341*, 197−205.
Breslow, R., & Chapman, W. H., Jr. (1994) *Proc. Natl. Acad. Sci. U.S.A. 93*, 10018−10021.
Brünger, A. T. (1992) *Nature 355*, 472−475.
Brünger, A. T., Karplus, M., & Petsko, G. A. (1989) *Acta Crystallogr. A45*, 50−61.
Bruzik, K. S., & Tsai, M.-D. (1994) *Bioorg. Med. Chem. 2*, 49−72.
Bruzik, K. S., Morocho, A. M., Jhon, D.-Y., Rhee, S. G., & Tsai, M.-D. (1992) *Biochemistry 31*, 5183−5193.
Bruzik, K. S., Hakeem, A. A., & Tsai, M.-D. (1994) *Biochemistry 33*, 8367−8374.
Bullock, T. L., Ryan, M., Kim, S. L., Remington, S. J., & Griffith, O. H. (1993) *Biophys. J. 64*, 784−791.
Camilli, A., Goldfine, H., & Portnoy, P. A. (1991) *J. Exp. Med. 173*, 751−754.
Cheng, H.-F., Jiang, M.-J., Chen, C.-L., Liu, S.-M., Wong, L.-P., Lomasney, J. W., & King, K. (1995) *J. Biol. Chem. 270*, 5495−5505.
Corey, D. R., & Craik, C. S. (1992) *J. Am. Chem. Soc. 114*, 1784−1790.
Daugherty, S., & Low, M. G. (1993) *Infect. Immun. 61*, 5078−5089.
Ellis, M. V., U. S., & Katan, M. (1995) *Biochem. J. 307*, 69−75.
Essen, L.-O., Perisic, O., Cheung, R., Katan, M., & Williams, R. L. (1996) *Nature 380*, 595−602.
Essen, L.-O., Perisic, O., Katan, M., Wu, Y., Roberts, M. F., & Williams, R. L. (1997) *Biochemistry 36*, 1704−1718.
Ferguson, M. A. J., & Williams, A. F. (1988) *Annu. Rev. Biochem. 57*, 285−320.
Griffith, O. H., Volwerk, J. J., & Kuppe, A. (1991) *Methods Enzymol. 197*, 493−502.
Guther, M. L. S. Cardoso de Almeida, M. L., Rosenberry, T. L., & Ferguson, M. A. J. (1994) *Anal. Biochem. 219*, 249−255.
Heinz, D. W., Ryan, M., Bullock, T., & Griffith, O. H. (1995) *EMBO J. 14*, 3855−3863.
Ikezawa, H., & Taguchi, R. (1981) *Methods Enzymol. 71*, 731−741.
Ikezawa, H., Yamanegi, M., Taguchi, R., Miyashita, T., & Ohyabu, T. (1976) *Biochim. Biophys. Acta 450*, 154−164.
Jones, T. A., Zhou, J.-Y., Cowan, S., & Kjeldgaard, M. (1991) *Acta Crystallogr. A74*, 110−119.
Kabsch, W. (1988) *J. Appl. Crystallogr. 21*, 67−71.
Koke, J. A., Yang, M., Henner, D. J., Volwerk, J. J., & Griffith, O. H. (1991) *Protein Expression Purif. 2*, 51−58.
Kraulis, P. J. (1991) *J. Appl. Crystallogr. 24*, 946−950.
Kunkel, T. A., Roberts, J. D., & Zakour, R. A. (1987) *Methods Enzymol. 154*, 367−382.
Leigh, A. J., Volwerk, J. J., Griffith, O. H., & Keana, J. F. W. (1992) *Biochemistry 31*, 8979−8983.
Leimeister-Wächter, M., Domann, E., & Chakraborty, T. (1991) *Mol. Microbiol. 5*, 361−366.
Lewis, K. A., Garigapati, V. R., Zhou, C., & Roberts, M. F. (1993) *Biochemistry 32*, 8836−8841.
Low, M. G. (1981) *Methods Enzymol. 71*, 741−746.
Low, M. G., & Saltiel, A. R. (1988) *Science 239*, 268−275.
Martin, S. F., & Wagman, A. S. (1996) *J. Org. Chem. 61*. 8016−8023.
Mengaud, J., Braun-Breton, C., & Cossart, P. (1991) *Mol. Microbiol. 5*, 367−372.
Meyer, J. E. W. (1997) Ph.D. Thesis, University of Freiburg, Germany.
Morris, A. L., MacArthur, M. W., & Thornton, J. N. (1992) *Proteins: Struct.. Funct., Genet. 12*, 345−364.
Navaza, J. (1994) *Acta Crystallogr. D50*, 157−163.
Rhee, S. G., Suh, P.-G., Ryu, S. H., & Lee, S. Y. (1989) *Science 244*, 546−550.
Richards, F. M., & Wyckoff, H. W. (1971) in *The Enzymes* (Boyer, P. D., Ed.) pp 647−806, Academic Press, New York.
Ryan, M., Smith, M. P., Vinod, T. K., Lau, W. L., Keana, J. F. W., & Griffith, O. H. (1996) *J. Med. Chem. 39*, 4366−4376.
Shashidhar, M. S., Volwerk, J. J., Griffith, O. H., & Keana, J. F. W. (1991) *Chem. Phys. Lipids 60*, 101−110.
Taguchi, R., & Ikezawa, H. (1978) *Arch. Biochem. Biophys. 186*, 196−201.
Thompson, J. E., & Raines, R. T. (1994) *J. Am. Chem. Soc. 116*, 5467−5468.
Trakhanov, S., & Quiocho, F. A. (1995) *Protein Sci. 4*, 1914−1919.
Volwerk, J. J., Shashidhar, M. S., Kuppe, A., & Griffith, O. H. (1990) *Biochemistry 29*, 8056−8062.
Vriend, G., & Sander, C. (1993) *J. Appl. Crystallogr. 26*, 47−60.

BI971102D